

New copper corrosion inhibitors in chloride environments based on benzo-[1,2,4]-triazolo-[1,2]-triazinones

D.S. Shevtsov,¹ M.N.M. Mawlood,¹ O.A. Kozaderov,¹ Kh.S. Shikhaliev,^{1*}
A.A. Kruzhilin,^{1,2} A.Yu. Potapov,¹ I.D. Zartsyn¹ and Ch. Prabhakar³

¹Voronezh State University, 1 Universitetskaya pl., 394018 Voronezh, Russian Federation

²Voronezh State Agricultural University named after Emperor Peter I, 1 ul. Michurina,
394087 Voronezh, Russian Federation

³National Institute of Technology Kurukshetra, 136119 Kurukshetra, India

*E-mail: shikh1961@yandex.ru

Abstract

New compounds based on benzo[1,2,4]-triazolo[1,2,4]-triazinones have been synthesized in yields above 78%. The structures were confirmed by IR and ¹H NMR spectroscopy. For structures that can exist in tautomeric forms, the calculation of the total energy of the molecule shows the predominant realization of the keto form. A set of field tests, electrochemical, and quantum-chemical methods was used to evaluate the inhibition of copper corrosion in chloride environments. The lack of an inhibitory effect of benzo[e][1,2,4]triazolo[5,1-c][1,2,4]triazin-6-ol can be explained by excessive acidity due to the strong electron-acceptor properties of the triazolotriazine cycle. There was an increase in the degree of protection of up to 68% in 3% HCl solution for the modified 8,8-dimethyl-8,9-dihydrobenzo[e][1,2,4]triazolo[5,1-c][1,2,4]triazin-6(7*H*)-ones at a concentration of 1.00 mM in the series of substituents: “ethylsulfinyl–methyl–methylmercapto” with a maximum degree of protection observed for the structure without a substituent. In the neutral chloride solution, the highest degree of protection (93%) was obtained for 8,8-dimethyl-8,9-dihydrobenzo[e][1,2,4]triazolo[5,1-c][1,2,4]triazin-6(7*H*)-one. The difference in the results between the experiments when immersed in a neutral solution and in the salt fog chamber is explained by the possible mechanical washing away of the inhibitor from the metal surface during surface irrigation, which is typical of a salt fog chamber. It was suggested that the inhibitory effect is associated with the formation of chelate complexes due to the hydroxybenzotriazine fragments in the studied compounds.

Keywords: copper, corrosion inhibitors, chlorides, triazole derivatives, triazolotriazines.

Received: January 22, 2021. Published: February 10, 2021

doi: [10.17675/2305-6894-2021-10-1-13](https://doi.org/10.17675/2305-6894-2021-10-1-13)

Introduction

Today, application of corrosion inhibitors is one of the simplest and most cost-effective methods of corrosion protection, including in acidic media. Equipment based on copper and its alloys is used in various industries: machines for large power plants (nuclear and heat power plants, radio engineering complexes, civil and naval vessels), machines at chemical plants and oil refineries, as well as microelectronics and instrument engineering products.

Therefore, a significant number of recent publications are devoted to the synthesis and study of the effectiveness of the protective effect of organic compounds on non-ferrous metals in neutral and acidic media.

Heterocyclic compounds such as azoles have been widely used for protecting non-ferrous metals from corrosion [1]. The most common and the most studied azole-type inhibitors include 1,2,3-benzotriazole, its substituted analogues, and 3-aminotriazole derivatives [2]. Their advantage is the ability to protect copper and its alloys both in a neutral medium, including aggressive atmosphere, and in acid solutions [3, 4].

In recent years, inhibiting properties of condensed polyheterocyclic compounds are of particular interest, including those containing a triazole moiety as an articulated cycle. What is more, the majority of studies are devoted to steel passivation [5–7].

Consequently, it seems promising to research anticorrosive properties of a series of benzo-[1,2,4]-triazolo-[1,2,4]-triazines containing a hydroxyl group in the 6th position and combining in their structure an explicit moiety of 1*H*-1,2,4-triazole and hydroxybenzotriazine, a hidden analogue of 8-hydroxyquinoline. The study of the inhibiting effect of 8-hydroxyquinoline derivatives has involved quantum chemical calculations, modelling and field test corrosion experiments [8–12].

It is known that compounds containing a moiety of 8-hydroxyquinoline are capable of forming stable films on the metal surface due to the formation of chelate bonds with metal atoms. The inhibition of dissolved metals leads to the formation of complexes, which, in their turn, form protective layers that prevent further corrosion. This barrier blocks the active sites on the surface from further dissolution, thereby suppressing corrosion [13–15].

This work continues the investigation of the inhibitory effect of various aminotriazole derivatives [16–18]. The purpose of the paper is to study the inhibitory effect of substituted benzo-[1,2,4]-triazolo-[1,2,4]-triazines with regard to copper corrosion in acidic chloride environments and atmospheric corrosion, as well to establish the dependency of inhibitors' effectiveness on the electronic nature of the substituent in the side chain.

Experimental

Benzo[*e*][1,2,4]triazolo[5,1-*c*][1,2,4]triazin-6-ol (**a**) was synthesised using the method described in [19]. 2-*R*-8,8-dimethyl-8,9-dihydrobenzo[*e*][1,2,4]triazolo[5,1-*c*][1,2,4]triazin-6(7*H*)-ones (**b–e**) were synthesized by the condensation of 3-*R*-1*H*-1,2,4-triazole-5-diazonium salts with 5,5-dimethyl-1,3-cyclohexanedione (Figure 1).

General procedure for the synthesis of 2-*R*-8,8-dimethyl-8,9-dihydrobenzo[*e*][1,2,4]triazolo[5,1-*c*][1,2,4]triazin-6(7*H*)-ones (**b–e**).

To a stirred mixture of 5 mM of the corresponding 3-*R*-5-amino-1*H*-1,2,4-triazole, 5 cm³ of H₂O, and 13 mM of concentrated H₂SO₄, which had been cooled to 0°C, a 5% aqueous solution of 5 mM NaNO₂ was added drop by drop at such a rate that the temperature of the reaction mixture did not exceed 5°C. The solution was kept at this temperature for 5 minutes and added in portions to the cooled to 10°C mixture of 0.65 g of 5,5-dimethyl-1,3-cyclohexanedione, 5 g of AcONa, 2 cm³ of EtOH, and 40 cm³ of H₂O. The reaction mixture

was stirred for 3 hours. The precipitate of the reaction product was filtered, washed with H₂O, and air dried.

8,8-Dimethyl-8,9-dihydrobenzo[*e*][1,2,4]triazolo[5,1-*c*][1,2,4]triazin-6(7*H*)-one (**b**). Yield: 78%, mp: 181–183°C, ¹H NMR spectrum (DMSO-*d*₆), (δ, ppm, *J*/Hz): 1.15 (6H, 2CH₃), 2.65 (2H, CH₂), 5.66 (1H, CH=COH), 8.07 (1H, CH-triazole), 13.00 (1H, OH).

2,8,8-Trimethyl-8,9-dihydrobenzo[*e*][1,2,4]triazolo[5,1-*c*][1,2,4]triazin-6(7*H*)-one (**c**). Yield: 81%, mp: 192–194°C, ¹H NMR spectrum (DMSO-*d*₆), (δ, ppm, *J*/Hz): 1.13 (6H, 2CH₃), 2.28 (3H, CH₃-triazole), 2.63 (2H, CH₂), 5.44 (1H, CH=COH), 12.80 (1H, OH).

8,8-Dimethyl-2-(methylmercapto)-8,9-dihydrobenzo[*e*][1,2,4]triazolo[5,1-*c*][1,2,4]triazin-6(7*H*)-one (**d**). Yield: 80%, mp: 196–198°C, ¹H NMR spectrum (DMSO-*d*₆), (δ, ppm, *J*/Hz): 1.14 (6H, 2CH₃), 2.56 (3H, CH₃S), 2.64 (2H, CH₂), 5.55 (1H, CH=COH), 12.96 (1H, OH).

2-(Ethylsulfinyl)-8,8-dimethyl-8,9-dihydrobenzo[*e*][1,2,4]triazolo[5,1-*c*][1,2,4]triazin-6(7*H*)-one (**e**). Yield: 89%, mp: 203–205°C, ¹H NMR spectrum (DMSO-*d*₆), (δ, ppm, *J*/Hz): 1.14–1.17 (9H, 3CH₃), 2.66 (2H, CH₂), 3.11–3.16 (1H, CH₂S), 3.21–3.26 (1H, CH₂S), 5.77 (1H, CH=COH), 13.15 (1H, OH).

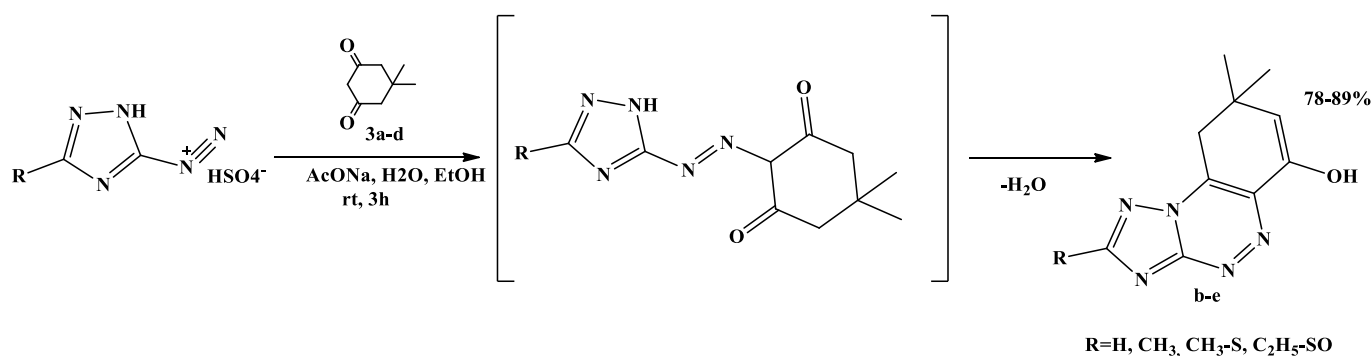


Figure 1. Synthesis scheme.

To evaluate the efficiency of the corrosion inhibition properties of the studied compounds, a set of electrochemical and field corrosion testing methods was used. Quantum-chemical calculations were also performed.

Electrochemical measurements were performed at room temperature (~25°C) on copper (M1) electrodes in an unstirred borate buffer aqueous solution (pH 7.4) with natural aeration, in the presence of the inhibitor and 10 mM NaCl. A classical electrolytic three-electrode cell was used in order to accelerate transient measurements.

A saturated silver chloride reference electrode was placed in a separate container linked to the electrolytic cell by an agar-agar-based salt bridge filled with a potassium nitrate saturated solution. The auxiliary electrode was a platinum gauze. The working copper electrode was polished by K3000 sandpaper, degreased in 96% ethanol, and washed with distilled water. The potentials of the working electrode (*E*) are given according to the standard hydrogen electrode (SHE) scale. The current density *i* was calculated by dividing the actual current *I* by the geometric area of the working electrode (0.75 cm²).

Electrochemical measurements were performed using an IPC-PRO potentiostat. In order to remove an oxide film, the working Cu-electrode was cathodically pre-polarised at $E = -0.60$ V for 15 minutes prior to the experiment. The electrode was then held in the solution for about 3 to 5 minutes until the corrosion potential (E_{cor}) stabilized. An NaCl solution was then added to the working solution while stirring, so that the concentration of chloride ions would be $C_{\text{Cl}^-} = 10$ mM. The studied inhibitors were also added to the solution in the concentration of $C_{\text{inh}} = 0.01, 0.10$ and 1.00 mM. After the new E_{cor} value was established, the polarisation curve was registered by scanning the potential towards either the anode or the cathode at 0.2 mV/sec. The activation potential (E_{act}) was identified by a rapid increase in the current on the anode polarisation curve. Pits were then visually identified on the surface of the electrode. The measurement error for E_{act} was below 0.03 V.

The rate of corrosion in current units (i_{cor}) was determined by the polarisation resistance technique as summarized by Mansfeld [20].

The effectiveness of the inhibition activity of the substituted benzo-[1,2,4]-triazolo-[1,2,4]-triazines (**a–e**) was evaluated judging by the degree of protection:

$$Z_i = \frac{i_{\text{cor},0} - i_{\text{cor,inh}}}{i_{\text{cor},0}} \cdot 100\%,$$

where $i_{\text{cor},0}$ and $i_{\text{cor,inh}}$ are the corrosion current densities with and without the inhibitor respectively.

A field corrosion testing was carried out on copper plates with a surface area of $S = 20 \times 50$ mm² and a thickness of $d = 0.10$ mm, which were preliminarily polished with K3000 sandpaper and degreased in acetone. Inhibitor protective films were obtained by keeping the copper plates in an aqueous solution with the inhibitor for 60 minutes at 25°C .

The experiments, which lasted $t = 7$ days, were carried out on three samples in an unstirred naturally aerated 1% HCl solution all at the same time. The plates were then washed with distilled water and treated according to GOST 9.907-83 “Methods for the removal of corrosion products after corrosion tests”. The rate of corrosion was determined according to the weight loss of the samples and calculated using the equation:

$$k = \frac{m_0 - m}{S \cdot t} \cdot 100\%,$$

where m_0 and m is the weight of the sample before and after the corrosion tests respectively.

The inhibitory effect of 3-alkyl-5-amino-1*H*-1,2,4-triazoles was evaluated by the value of the inhibition factor:

$$\gamma = \frac{k_0}{k_{\text{inh}}},$$

and the degree of protection:

$$Z_k = \frac{k_0 - k_{\text{inh}}}{k_0} \cdot 100\%,$$

where k_0 and k_{inh} are the rates of corrosion in the HCl solution with and without the inhibitor respectively. The parameter k_0 was $20 \text{ g} \cdot \text{m}^{-2} \cdot \text{day}^{-1}$.

The atmospheric corrosion of copper was accelerated by means of a salt spray testing in order to determine the inhibition effect of substituted benzo-[1,2,4]-triazolo-[1,2,4]-triazines (**a–e**) for inter-operational protection of copper products. The samples were dried and placed in a chamber at 95–100% air humidity. A 5% NaCl solution (pH 6.5–7.2, GOST R 52763-2007) was sprayed into the chamber every hour. The samples were examined three times every 24 hours to determine the time when the first signs of corrosion (τ_{cor}) occurred.

The optimisation of the geometry of the studied inhibitor molecules was carried out within the framework of the density functional theory (DFT) using the B3LYP functional with basis 6-311+ G(d,p) in the Gaussian 09 package [21]. The optimised geometry of molecules is characterised by a lack of negative oscillation frequencies and therefore corresponds to the minimum value on the potential energy surface. In addition, TDDFT calculations for optimised geometry were performed to find the five lowest electronic excitations. Frontier molecular orbitals were used to predict the effectiveness of inhibiting molecules. Within the limitation of the Koopmans' theorem, the energies of frontier orbitals are determined by the equation [22]:

$$-E_{\text{HOMO}} = IP \text{ and } -E_{\text{LUMO}} = EA$$

where IP is ionisation potential, and EA is electron affinity. Chemical hardness (η) is calculated by the following equation [22]:

$$\eta = \frac{IP - EA}{2}.$$

Softness (σ) is defined as a reciprocal value and is calculated as follows:

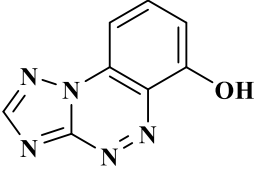
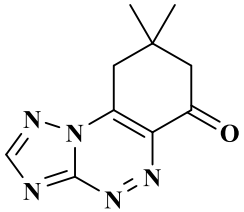
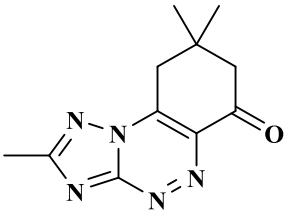
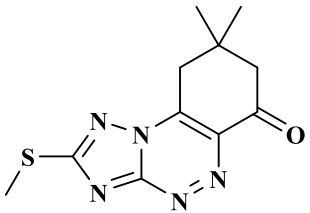
$$\sigma = \frac{1}{\eta}$$

Results and Discussion

The structural formulas and the solubility of the studied substances in water are shown in Table 1. Tricyclic condensed structures with enol (**a**) and keto functional groups (**b–e**) were studied, as well as the influence of the electronic nature of the substituent in the aminotriazole cycle. It should be noted that in solutions the compounds (**b–e**) may exist in two tautomeric forms (ketonic and enol), and thus they also contain a moiety of 8-hydroxyquinoline (Figure 2).

The analysis of polarisation curves shows that the addition of 0.01 mM of **a**, **d**, and **e** shifts E_{cor} of up to 30 mV in the anodic direction compared to the test experiment without organic additives (Table 2). The introduction of a similar concentration of **b** shifts E_{cor} in the anode region of up to ≈ 60 mV, whereas in case of **c** there is a shift in the cathode region of up to 80 mV. An increase in the additive concentration has different effects on E_{cor} : for **a** the values were similar to those of the test experiment, for **b** there was a shift in the cathode region of 60–67 mV, for **d** and **e** the change was insignificant and did not exceed ± 10 mV, whereas for **c** there was an increase and a shift in the anode region of up to 26 mV at $C_{\text{inh}}=0.10$ mM and up to 100 mV at $C_{\text{inh}}=1.00$ mM. In case of a protective effect, compounds **a**, **d**, and **e** can be considered as mixed-type inhibitors [23], compounds **b** and **c** depending on concentration, predominantly affect the cathodic or anodic half-reaction.

Table 1. Compound names, structures and solubility in water.

Symbol	Name	Formula	Solubility, $\text{mol}\cdot\text{dm}^{-3}$
a	Benzo[e][1,2,4]triazolo[5,1-c][1,2,4]triazin-6-ol		$2.2\cdot 10^{-3}$
b	8,8-Dimethyl-8,9-dihydrobenzo[e][1,2,4]triazolo[5,1-c][1,2,4]triazin-6(7H)-one		$5.0\cdot 10^{-3}$
c	2,8,8-Trimethyl-8,9-dihydrobenzo[e][1,2,4]triazolo[5,1-c][1,2,4]triazin-6(7H)-one		$2.5\cdot 10^{-3}$
d	8,8-Dimethyl-2-(methylmercapto)-8,9-dihydrobenzo[e][1,2,4]triazolo[5,1-c][1,2,4]triazin-6(7H)-one		$3.8\cdot 10^{-3}$

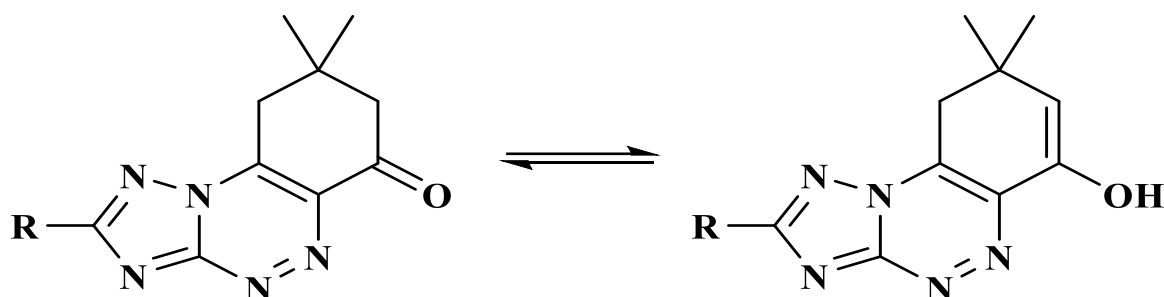
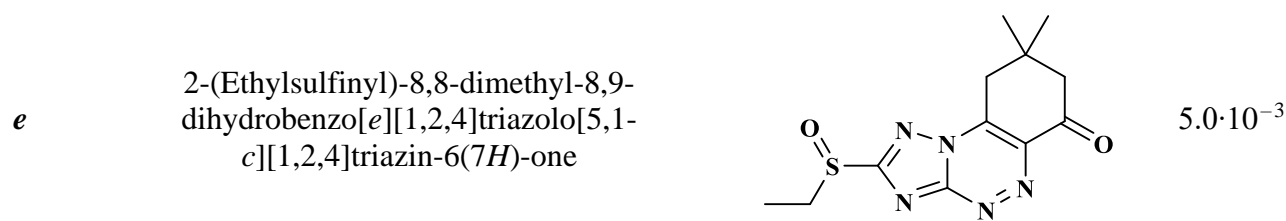


Figure 2. Tautomeric forms of compounds *b–e*.

Table 2. Open circuit potential, polarisation resistance, corrosion current density, and degree of protection of copper electrode in 0.01 M NaCl solutions with different derivatives of benzo-[1,2,4]-triazolo-[1,2,4]-triazinones.

Compound	Concentration of inhibitor, C_{inh} , mM	Corrosion potential, E_{cor} , V	Polarisation resistance, R_p , $k\Omega \cdot cm^2$	Corrosion rate, i_{cor} , $\mu A \cdot cm^{-2}$	Degree of protection, Z_i , %
None	–	0.172	41.9±4.6	1.2±0.3	–
<i>a</i>	0.01	0.206	38.9±5.6	1.7±0.3	–41.7
	0.10	0.170	49.5±2.3	1.10±0.24	8.3
<i>b</i>	0.01	0.236	43.2±4.5	1.13±0.36	5.8
	0.10	0.105	226±55	0.13±0.03	89.2
	1.00	0.112	492±88	0.08±0.03	93.3
<i>c</i>	0.01	0.092	91.2±29.2	0.60±0.17	50.0
	0.10	0.198	138.6±49.0	0.47±0.12	60.8
	1.00	0.275	152.7±14.0	0.35±0.13	70.8
<i>d</i>	0.01	0.198	90.0±14.2	0.86±0.17	28.3
	0.10	0.203	96.2±8.1	0.81±0.04	32.5
	1.00	0.184	93.3±13.5	0.73±0.14	39.2
<i>e</i>	0.01	0.198	112.1±17.8	0.95±0.28	20.8
	0.10	0.192	71.6±16.8	0.78±0.17	35.0
	1.00	0.196	72.6±13.3	0.72±0.20	40.0

On the anodic polarisation curves for all the studied concentrations of **a** (Figure 3a, curves 2–4), the maximum current density was formed in the potential region of 0.25–0.35 V, whose height exceeded the value for the test experiment. At $C_{\text{inh}}=0.10\text{--}1.00\text{ mM}$, E_{act} shifted in the positive direction up to 120–150 mV (Figure 3a, curves 3, 4). The cathodic polarisation curves were close to the curve of the test experiment (Figure 3a, curves 1'–4').

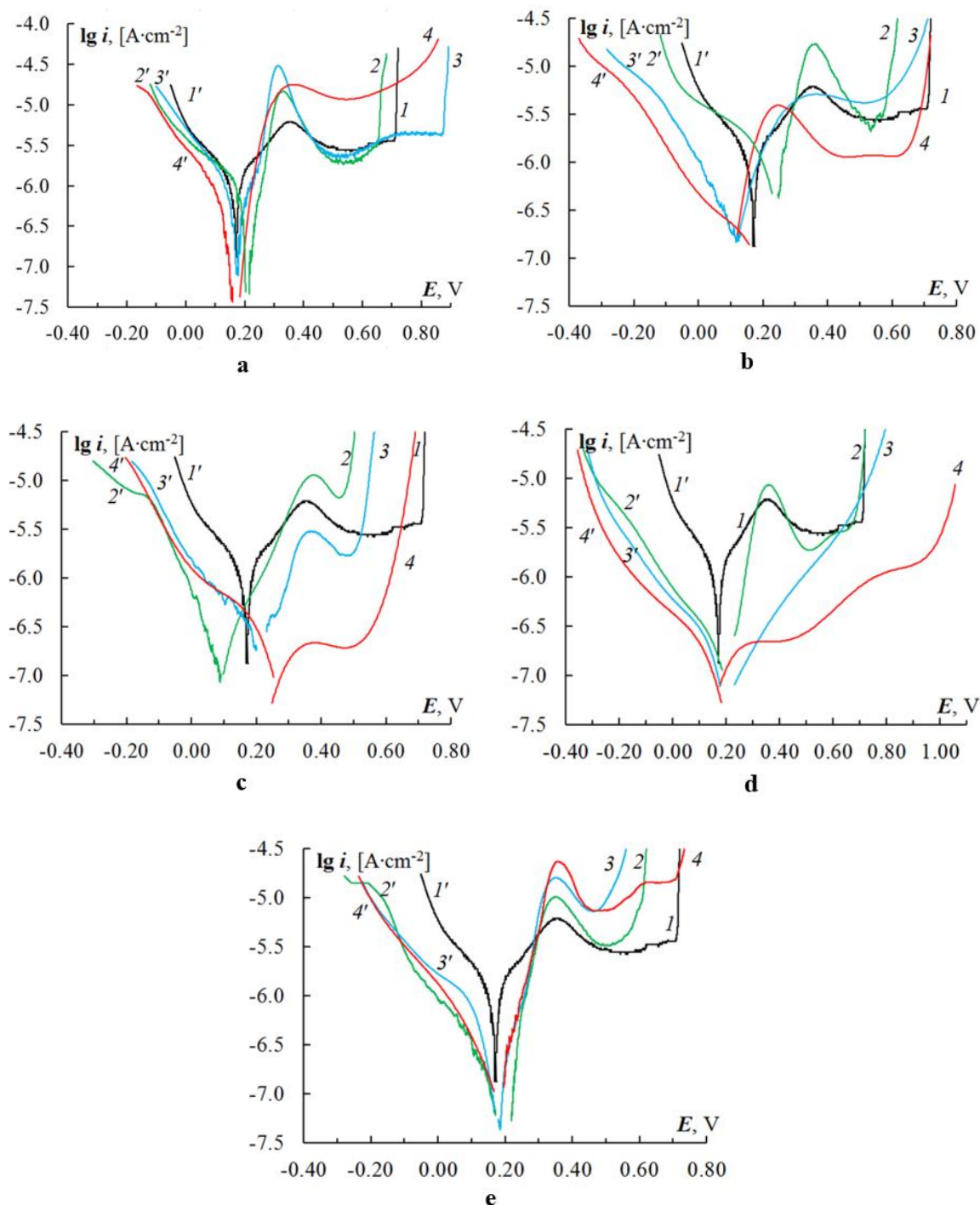


Figure 3. Anodic (1–4) and cathodic (1'–4') polarisation curves of copper in borate buffer (pH 7.4) +10 mM NaCl without an inhibitor (I , I') and in presence of compound **a** (a),

compound **b** (*b*), compound **c** (*c*), compound **d** (*d*), compound **e** (*e*) at concentrations of 0.01 (2), 0.10 (3), and 1.00 mM (4).

For compounds **b**, **c**, and **d** there were similar variations in the initial section of the anodic polarisation curves (Figure 3*b–d*). At $C_{inh}=0.01$ mM, the maximum current density exceeded the control value (Figure 3*b–d*, curve 2). As a result of an increase in C_{inh} up to 0.10–1.00 mM (Figure 3*b–d*, curves 3, 4) the values of maximum current density were below the reference value (for **d** a maximum was not formed). The peak shifted in the cathodic direction to 50–100 mV. With an increase in C_{inh} , the E_{act} values shifted in the anodic direction, however, they did not exceed the result of the test experiment, with the exception of **d** at $C_{inh}=1.00$ mM. The current density on the cathodic polarisation curves at equal values of the electrode potential in the presence of the additives **b**, **c**, and **d** was by up to $\frac{1}{2}$ order of magnitude less than in the test experiment (Figure 3*b–d*, curve 2'–4'). Only for **b** at $C_{inh}=0.01$ mM the difference was insignificant.

On the anodic polarisation curves for **e**, the maximum current in the region of active dissolution gradually increased with an increase in concentration. It also exceeded the result of the reference measurement in all cases (Figure 3*e*, curves 2–4). The activation potential shifted in the anodic direction, however, it did not exceed the reference value. The cathodic polarisation curves pressed against the current axis and at equal values of the electrode potential the current density (absolute value) was less than the reference value (Figure 3*e*, curves 2'–4'). A change in the concentration within 0.01–1.00 mM did not cause any noticeable changes in the shape and the position of cathodic polarisation curves.

Thus, based on the data presented on the total polarisation curves it was established that within the concentration of 0.01–1.00 mM the introduction of substance **a** does not lead to a significant reduction in current density at similar values of the electrode potential. For substance **b**, with an increase in C_{inh} there is a decrease in the current density in the anodic and cathodic sections of polarisation curves. An increase in the concentration of additives **c** and **d** results in a gradual decrease in the current density on the anodic polarisation curves. The reduction of the current density for cathodic polarisation curves is similar for all concentrations. The introduction of **e** only reduces the current density on the cathodic polarisation curves in a similar way for all concentrations of the substance.

Calculations of the corrosion rate of copper near E_{cor} by polarisation resistance technique established that the addition of **a** at $C_{inh}=0.01$ mM can lead to an intensified corrosion process in a neutral chloride solution (Table 1). With an increasing concentration, the degree of protection does not exceed 10%. For **e**, **d**, and **c** an increase in concentration leads to a gradual increase in the degree of protection from 20% to 40%, from 28% to 39%, and from 50% to 70% respectively. The highest degree of protection (83–93%) was obtained for the compound **b** at $C_{inh}=0.10$ –1.00 mM. At the lowest concentration Z_i does not exceed 6%.

Testing in a salt spray chamber (Table 3) showed the results which are similar to the experiments in aqueous solutions. For **a** there was an increase in τ_{cor} of no more than 4–5

hours compared to the test experiment for concentrations of 0.1 and 1.0 mM, whereas for *e* there was an increase in τ_{cor} of 6–9 hours, for *c* it was 24–30 hours, and for *d* it was 51–60 hours. For *b* barely any increase in τ_{cor} was observed. The authors associate the discrepancies between the results for *b* with the impact of environmental exposure during the tests. In case of spraying metal plates with the solution, there is a mechanical influence by the solution's particles and the inhibitor might be washed away from the metal surface due to the lower adsorption energy.

Table 3. Results of the copper natural corrosion tests.

Compound	Concentration of inhibitor C_{inh} , mM	Corrosion rate k , $\text{g}\cdot\text{m}^{-2}\cdot\text{day}^{-1}$	Inhibition coefficient, γ	Degree of protection Z_k , %	Time to corrosion τ_{cor} , h
None	–	20.0	–	–	1–2
<i>a</i>	0.01	20.2	0.9	–1.0	2
	0.10	19.5	1.0	2.5	6
	1.00	19.2	1.1	7.4	6
<i>b</i>	0.01	16.3	1.2	18.5	2
	0.10	9.2	2.2	54.0	2
	1.00	6.4	3.2	68.0	4
<i>c</i>	0.01	21.1	0.9	–5.5	26
	0.10	16.6	1.2	17.0	28
	1.00	13.6	1.5	32.7	32
<i>d</i>	0.01	18.4	1.1	8.0	53
	0.10	13.3	1.5	33.5	62
	1.00	12.4	1.6	37.8	53
<i>e</i>	0.01	18.9	1.1	5.6	8
	0.10	17.2	1.2	14.0	10
	1.00	14.7	1.4	26.6	10

The external appearance of copper plates after 20 hours of exposure in the salt spray chamber, preceded by their exposure to the solution with the addition of compound *c*, is shown in Figure 4. The samples without inhibitor treatment (Figure 4*b*) were covered with a layer of corrosion products of a dark brown colouring. The plates that were treated with inhibitors *c* and *d* demonstrated no visible changes compared to their initial state or had a slight yellow staining. The samples treated with compounds *a*, *b*, *e* had corrosion centres and there was a darkening of the metal.

The results of the test in an acid chloride environment are similar in nature to the experiments in aqueous electrolyte solutions. The lowest degree of protection at $C_{inh}=1.0$ mM was obtained for compound **a** (7.4%). There was an increase in the degree of protection in the series of compounds **e–c–d–b** (26.6–32.7–37.8–68.0%, respectively), *i.e.*, there was only a discrepancy with regard to the position of **c** and **d**.

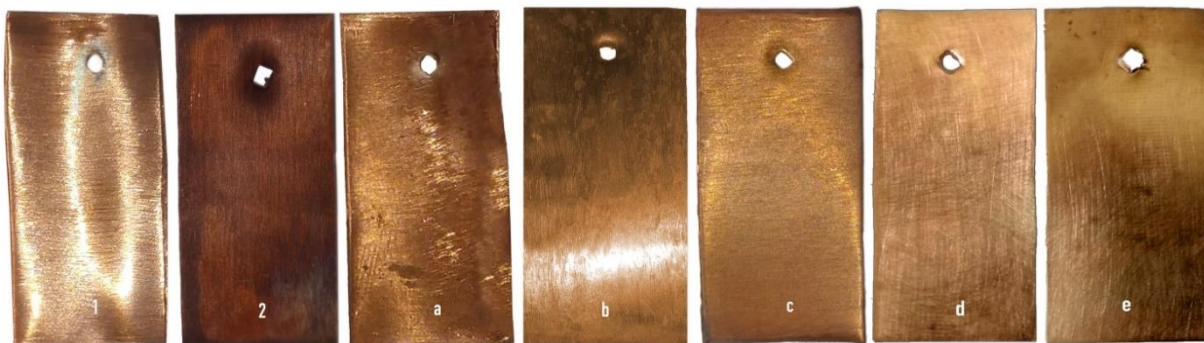


Figure 4. Copper samples before (1) and after salt spray corrosion testing without an inhibitor (2), and in the presence of compound **a** (a), compound **b** (b), compound **c** (c), compound **d** (d), compound **e** (e) at concentrations of 1.00 mM.

The calculated values of pK_a for the studied compounds (Table 4) showed that in terms of the values of acidity the enol forms of compounds **b–e** were similar to the structure of the 8-hydroxyquinoline molecule. This also confirms their ability to form chelate protection complexes on a metal surface (Figure 5).

Table 4. Values of acidity constants.

Compound	The acidity constant, pK_a
8-hydroxyquinoline	10.109
a	6.912
b	9.819
c	9.811
d	9.788
e	9.505

Compound **a** may only exist in the hydroxyl (enol) form. Due to the strong electron-acceptor properties of the triazolotriazine cycle, it had a lower pK_a than that of 8-hydroxyquinoline and the rest of the studied compounds, which characterises this molecule as being a stronger acid. The increased acidity explains a decrease in the protective properties of this compound with respect to copper compared to other studied compounds. A decrease in the inhibitory properties of compound **e** can also be associated with an increase in acidity due to strong electron-acceptor properties of the methylsulphonyl group in [1]. As a result,

compounds **b**, **c**, and **d** should have the highest inhibitory properties, which correspond with the experimental results.

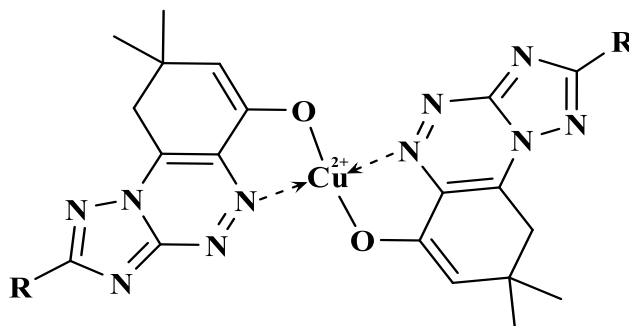


Figure 5. Chelate complexes based on 8-hydroxyquinoline derivatives with Cu^{2+} ions.

When conducting quantum chemical modelling, it was a priority to establish the most energetically favourable tautomeric state for compounds **b–e** which can exist in keto or enol forms. The optimised structures of the compounds obtained by quantum chemical modelling are shown in Figure 6. The calculations of the total energy of the molecule (Table 5) suggest that compounds **b–e** predominantly exist in keto form, however, they do not exclude the possibility of keto-enol tautomerism in the studied environments.

Table 5. Calculated energies of HOMO, LUMO, HOMO LUMO gaps (HLG), ionisation potential (*IP*), electron affinity (*EA*), electronegativity (χ), absolute hardness (η) and softness (σ) in eV at B3LYP/6-31 G (d, p) level.

Compound	Energy	HOMO	LUMO	HLG	<i>IP</i>	<i>EA</i>	χ	η	σ
a	−656.793	−6.71	−2.54	4.17	6.71	2.54	4.63	2.09	0.48
b -keto	−736.632	−6.90	−2.56	4.34	6.90	2.56	4.73	2.17	0.46
b -enol	−736.614	−6.17	−2.42	3.75	6.17	2.42	4.30	1.88	0.53
c -keto	−775.960	−6.77	−2.42	4.35	6.77	2.42	4.60	2.18	0.46
c -enol	−775.942	−6.01	−2.11	3.90	6.01	2.11	4.06	1.95	0.51
d -keto	−1174.140	−6.66	−2.46	4.20	6.66	2.46	4.56	2.10	0.48
d -enol	−1174.123	−6.05	−2.14	3.91	6.05	2.14	4.10	1.96	0.51
e -keto	−1288.618	−6.44	−2.85	3.59	6.44	2.85	4.65	1.80	0.56
e -enol	−1288.599	−6.26	−2.47	3.79	6.26	2.47	4.37	1.90	0.53

It is known that the ability of inhibitors to interact with a metal surface increases with an increase in HOMO and a decrease in LUMO [24]. The smaller the HOMO–LUMO gap, the higher the reactivity of the inhibitor to the metal surface and the stronger the inhibitory effect. Following this approach, according to the HOMO value, **b** should have the highest

protective effect, the effectiveness of **a**, **c**, and **d** should be similar, and **e** should be the least effective. However, due to the LUMO contribution and the HLG calculation, it would be more correct to assume an increase in the inhibitory effect in the series of compounds **e–a–d–c–b**. In practice similar results were obtained, with the exception of the positions of compounds **a** and **e**, which may be associated with the features of the systems analysed during the experiments that were not included in the calculations.

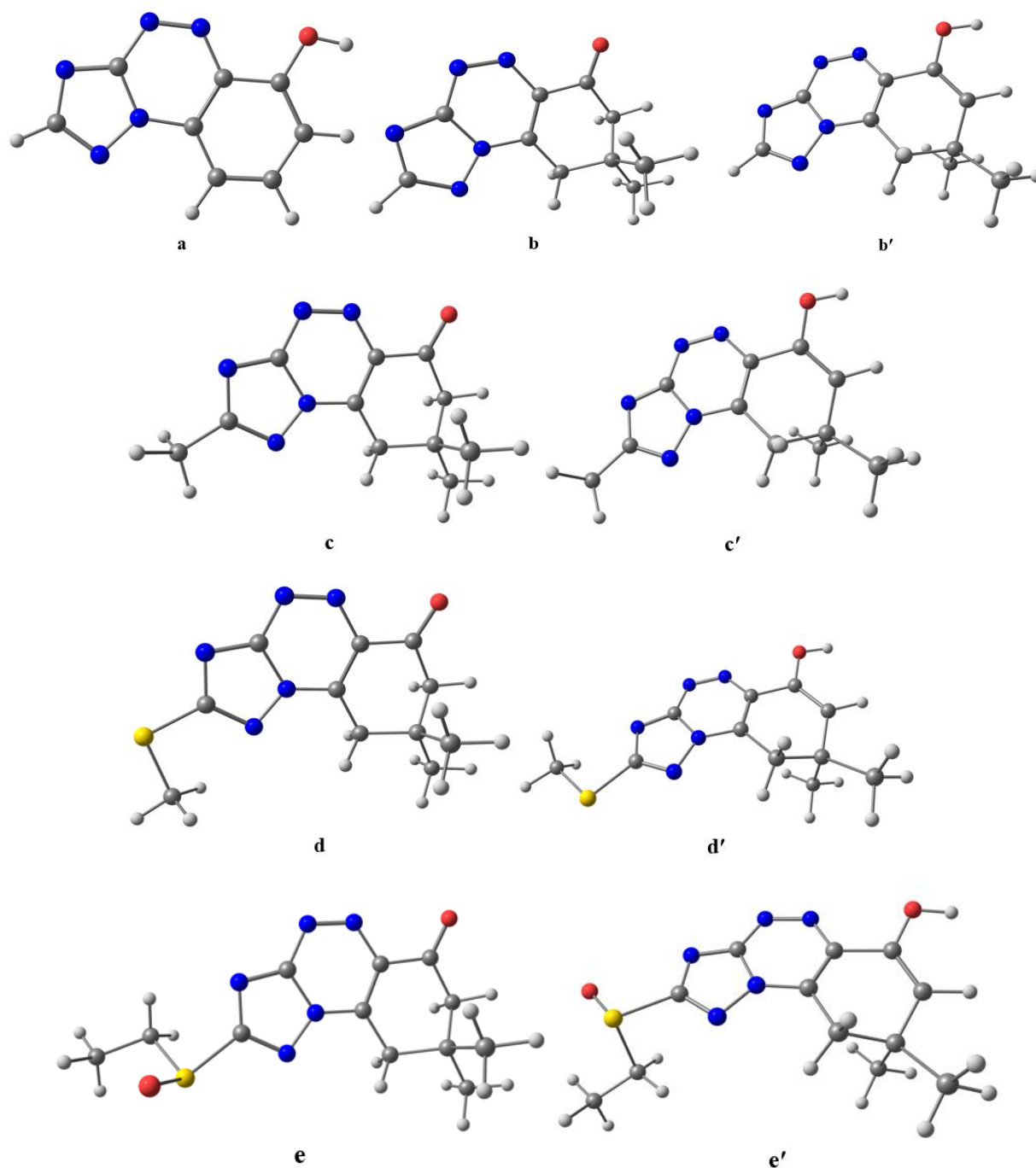


Figure 6. Optimised structures of the molecules considered for study (' – corresponds to the enol form)

The studied compounds must exhibit passivating properties similar to known examples of 8-hydroxyquinoline-based inhibitors due to the presence in their structure of such chelating hydroxybenzotriazine moiety capable of forming chelate complexes with 2-valent metal ions (Figure 5). This phenomenon is possible due to a juxtaposition of nitrogen endo atoms in the quinoline or triazine cycles and a hydroxyl group in the structure of the inhibitors which results in the highly protective properties of the studied compounds. [15, 25].

Conclusion

The inhibitory effect of benzo-[1,2,4]-triazolo-[1,2,4]-triazines with various substituents with respect to copper corrosion was evaluated using a set of electrochemical and direct corrosion tests, and quantum chemical modelling.

It was found that there is a lack of an inhibitory effect from benzo[*e*][1,2,4]triazolo[5,1-*c*][1,2,4]triazin-6-ol with respect to copper corrosion in neutral and hydrochloric acid solutions resulting from excessive acidity due to the strong electron-acceptor properties of the triazolotriazine cycle.

In the case of modified 8,8-dimethyl-8,9-dihydrobenzo[*e*][1,2,4]triazolo[5,1-*c*][1,2,4]triazin-6(7*H*)-ones at a concentration of 1.00 mM there is an increase in the degree of protection in 3% HCl solution of up to 68% in the series of substituents: “ethylsulfinyl–methyl–methylmercapto” with a maximum of the degree obtained for the structure without any substituent. In the neutral chloride solution, the highest degree of protection (93%) was also obtained for 8,8-dimethyl-8,9-dihydrobenzo[*e*][1,2,4]triazolo[5,1-*c*][1,2,4]triazine-6(7*H*)-one.

In the salt spray chamber, the highest protective effect was obtained for copper after immersing it in a solution of 8,8-dimethyl-2-(methylmercapto)-8,9-dihydrobenzo[*e*][1,2,4]triazolo[5,1-*c*][1,2,4]triazin-6(7*H*)-one with a concentration of 1.00 mM. The lack of protection for 8,8-dimethyl-8,9-dihydrobenzo[*e*][1,2,4]triazolo[5,1-*c*][1,2,4]triazin-6(7*H*)-one was explained by the possible “washing away” of the inhibitor as a result of spraying a saline solution during the tests.

The values of acidity constants and quantum chemical calculations confirm the higher inhibitory properties for 8,8-dimethyl-8,9-dihydrobenzo[*e*][1,2,4]triazolo[5,1-*c*][1,2,4]triazin-6(7*H*)-one and methyl-, methylmercapto-substituted structures compared to benzo[*e*][1,2,4]triazolo[5,1-*c*][1,2,4]triazin-6-ol. It was shown that in terms of the total energy of the molecule the keto form predominates over the enol form.

Acknowledgements

The study was supported by the Russian Foundation for Basic Research, project no. 20-33-80017.

References

1. Yu.I. Kuznetsov and L.P. Kazansky, Physicochemical aspects of metal protection by azoles as corrosion inhibitors, *Russ. Chem. Rev.*, 2008, **77**, no. 3, 219–232. doi: [10.1070/RC2008v077n03ABEH003753](https://doi.org/10.1070/RC2008v077n03ABEH003753)
2. Yu.I. Kuznetsov, *Organic inhibitors of corrosion of metals*, Springer Science & Business Media, 1996.
3. Yu. I. Kuznetsov, New possibilities of metal corrosion inhibition by organic heterocyclic compounds, *Int. J. Corros. Scale Inhib.*, 2012, **1**, no. 1, 3–15. doi: [10.17675/2305-6894-2012-1-1-003-015](https://doi.org/10.17675/2305-6894-2012-1-1-003-015)
4. Yu.B. Makarychev, I.A. Arhipushkin, Kh.S. Shikhaliev and L.P. Kazansky, Formation of nanolayers on the surface from aqueous solutions by some azoles. Part 2, *Korrozi. Mater., Zashch. (Corrosion: materials, protection)*, 2016, no. 4, 43–48 (in Russian).
5. S. Lahmidi, A. Elyoussfi, A. Dafali, H. Elmsellem, N.K. Sebbar, L.El. Ouasif, A.E. Jilalat, B.El Mahi, E.M. Essassi, I. Abdel-Rahman and B. Hammouti, Corrosion inhibition of mild steel by two new 1,2,4-triazolo[1, 5-*a*] pyrimidine derivatives in 1 M HCl: Experimental and computational study, *J. Mater. Environ. Sci.*, 2017, **8**, no. 1, 225–237.
6. Y.El Bakri, L. Guo, E.H. Anouar and E.M. Essassi, Electrochemical, DFT and MD simulation of newly synthesized triazolotriazepine derivatives as corrosion inhibitors for carbon steel in 1 M HCl, *J. Mol. Liq.*, 2019, **274**, 759–769. doi: [10.1016/j.molliq.2018.11.048](https://doi.org/10.1016/j.molliq.2018.11.048)
7. I.R. Saad, A.M. Abdel-Gaber, G.O. Younes and B. Nsouli, Corrosion Inhibition of Mild Steel in Acidic Solutions Using 1,2,4-triazolo[1,5-*a*] pyrimidine, *Russ. J. Appl. Chem.*, 2018, **91**, no. 2, 245–252. doi: [10.1134/S107042721802012X](https://doi.org/10.1134/S107042721802012X)
8. H. Lgaz, R. Salghi, K.S. Bhat, A. Chaouiki, and S. Jodeh, Correlated experimental and theoretical study on inhibition behavior of novel quinoline derivatives for the corrosion of mild steel in hydrochloric acid solution, *J. Mol. Liq.*, 2017, **244**, 154–168. doi: [10.1016/j.molliq.2017.08.121](https://doi.org/10.1016/j.molliq.2017.08.121)
9. A.S. Fouda, M.A. Ismael, R.M. Abo Shahba, L.A. Kamel and A.A. El-Nagggar, Corrosion inhibition of copper and α -brass in 1 M HNO₃ solution using new arylpyrimido[5,4-*c*]quinoline-2,4-dione derivative, *Int. J. Electrochem. Sci.*, 2017, **12**, 3361–3384. doi: [10.20964/2017.04.57](https://doi.org/10.20964/2017.04.57)
10. A. Elyoussfi, A. Dafali, H. Elmsellem, Y. Bouzian, R. Bouhfid, A. Zarrouk, K. Cherrak, E.M. Essassi, A. Aouniti and B. Hammouti, Some quinoline derivatives: synthesis and comparative study towards corrosion of mild steel in 0.5 H₂SO₄, *Der Pharma Chemica*, 2016, **8**, no. 4, 226–236.
11. H. About, M.El Faydy, Z. Rouifi, F. Benhiba, H. Ramsis, M. Boudalia, H. Zarrok, H. Oudda, R. Tourir, M.El M'Rabet, I. Warad, A. Guenbour and B. Lakhrissi, Experimental and theoretical studies of 5-((4-phenyl-4,5-dihydro-1H-tetrazol-1-yl)methyl)quinolin-8-ol quinoline derivative as effective corrosion inhibitor for mild

- steel in 1.0 M HCl, *J. Mater. Environ. Sci.*, 2018, **9**, no. 1, 345–357. doi: [10.26872/jmes.2018.9.1.38](https://doi.org/10.26872/jmes.2018.9.1.38)
12. A.S. Fouda, K.El-Shiekh, S.Abd El-Maksoud and M.A. Diab, 8-hydroxy-7-phenylazo-quinoline-5-sulfonic acid derivatives as corrosion inhibitors for copper in nitric acid solutions, *J. Electrochem. Plat. Technol.*, 2015. doi: [10.12850/ISSN2196-0267.JEPT5431](https://doi.org/10.12850/ISSN2196-0267.JEPT5431)
13. E. Bardez, I. Devol, B. Larrey and B. Valeur, Excited-state processes in 8-hydroxyquinoline: photoinduced tautomerization and solvation effects, *J. Phys. Chem. B*, 1997, **101**, no. 39, 7786–7793. doi: [10.1021/jp971293u](https://doi.org/10.1021/jp971293u)
14. E. Filip, I. Humelnicu and C. Ghirvu, Some aspects of 8-hydroxyquinoline in solvents, *Acta Chem. Iasi*, 2009, **17**, 85–96.
15. W. Liu, A. Singh, Y. Lin, E.E. Ebenso, L. Zhou and B. Huang, 8-Hydroxyquinoline as an effective corrosion inhibitor for 7075 aluminium alloy in 3.5% NaCl solution, *Int. J. Electrochem. Sci.*, 2014, **9**, 5574–5584.
16. D.S. Shevtsov, Kh.S. Shikhaliev, N.V. Stolpovskaya, A.A. Kruzhilin, A.Yu. Potapov, I.D. Zartsyn, O.A. Kozaderov, D.V. Lyapun, Ch. Prabhakar, A. Tripathi, 3-Alkyl-5-amino-1,2,4-triazoles synthesized from the fatty acids of sunflower oil processing waste as corrosion inhibitors for copper in chloride environments, *Int. J. Corros. Scale Inhib.*, 2020, **9**, no. 2, 726–744. doi: [10.17675/2305-6894-2020-9-2-21](https://doi.org/10.17675/2305-6894-2020-9-2-21)
17. O.A. Kozaderov, Kh.S. Shikhaliev, Ch. Prabhakar, D.S. Shevtsov, A.A. Kruzhilin, E.S. Komarova, A.Yu. Potapov and I.D. Zartsyn, Copper corrosion inhibition in chloride environments by 3-(*N*-hetaryl)-5-amino-1*H*-1,2,4-triazoles, *Int. J. Corros. Scale Inhib.*, 2019, **8**, no. 2, 422–436. doi: [10.17675/2305-6894-2019-8-2-19](https://doi.org/10.17675/2305-6894-2019-8-2-19)
18. O. Kozaderov, K. Shikhaliev, C. Prabhakar, A. Tripathi, D. Shevtsov, A. Kruzhilin, E. Komarova, A. Potapov, I. Zartsyn and Yu. Kuznetsov, Corrosion of α -Brass in Solutions Containing Chloride Ions and 3-Mercaptoalkyl-5-amino-1*H*-1,2,4-triazoles, *Appl. Sci.*, 2019, **9**, no. 14, 2821. doi: [10.3390/app9142821](https://doi.org/10.3390/app9142821)
19. M.N. Mawlood, A.Yu. Potapov, D.Yu. Vandyshev, Kh.S. Shikhaliev, M.A. Potapov, I.V. Ledenyova and E.A. Kosheleva, 1*H*-1,2,4-Triazolo-5-diazonium salts in the synthesis of novel [1,2,4]triazolo[1,5-*c*][1,2,4]benzotriazin-6-ols, *Chem. Heterocycl. Compd.*, 2019, **55**, 1075–1079. doi: [10.1007/s10593-019-02580-9](https://doi.org/10.1007/s10593-019-02580-9)
20. F. Mansfeld, Tafel slopes and corrosion rates obtained in the pre-Tafel region of polarisation curves. *Corros. Sci.*, 2005, **47**, no. 12, 3178–3186. doi: [10.1016/j.corsci.2005.04.012](https://doi.org/10.1016/j.corsci.2005.04.012)
21. M.J. Frisch, G.W. Trucks, H.B. Schlegel, G.E. Scuseria, M.A. Robb, J.R. Cheeseman, G. Scalmani, V. Barone, G.A. Petersson and H. Nakatsuji, *Gaussian 16 (Revision B.01)*, Gaussian, Inc.: Wallingford, 2016.
22. R.G. Parr and R.G. Pearson, Absolute hardness: Companion parameter to absolute electronegativity, *J. Am. Chem. Soc.*, 1983, **105**, no. 26, 7512–7516. doi: [10.1021/ja00364a005](https://doi.org/10.1021/ja00364a005)

-
23. N.A. Negm, M.F. Zaki, M.M. Said and S.M. Morsy, Inhibitory action of biodegradable modified vanillin on the corrosion of carbon steel in 1 M HCl, *Corros. Sci.*, 2011, **53**, no. 12, 4233–4240. doi: [10.1016/j.corsci.2011.08.034](https://doi.org/10.1016/j.corsci.2011.08.034)
 24. M. Özcan, I. Dehri, and M. Erbil, Organic sulphur-containing compounds as corrosion inhibitors for mild steel in acidic media: correlation between inhibition efficiency and chemical structure, *Appl. Surf. Sci.*, 2004, **236**, 155–164. doi: [10.1016/j.apsusc.2004.04.017](https://doi.org/10.1016/j.apsusc.2004.04.017)
 25. H. Gao, Q. Li, Y. Dao, F. Luo and H.X. Zhang, High efficiency corrosion inhibitor 8-hydroxyquinoline and its synergistic effect with sodium dodecylbenzenesulphonate on AZ91D magnesium alloy, *Corros. Sci.*, 2010, **52**, no. 5, 1603–1609. doi: [10.1016/j.corsci.2010.01.033](https://doi.org/10.1016/j.corsci.2010.01.033)

